Article

Solid Particle Erosion of Unfilled and Filled Epoxy Resin at Room and Elevated Temperatures

Maxim Mishnev [1,] *, Alexander Korolev [1,] *, Dmitriy Ulrikh [2], Anna Gorechneva [1], Denis Sadretdinov [1], Danila Grinkevich [1]

[1] Department of building construction and structures, South Ural State University, Chelyabinsk, 454080, Russia

[2] Department of town planning, engineering systems, and networks, South Ural State University, Chelyabinsk, 454080, Russia

* Correspondence: korolev@sc74.ru or korolevas@susu.ac.ru (A.K.); mishnevmv@susu.ru (M.M.); Tel.: +7-(922)-750-6508 (A.K.); +7-(999)-585-1936 (M.M.)

Abstract: The solid particle erosion at room and elevated temperatures of pure and filled hot-curing epoxy resin on anhydride hardener was experimentally tested using accelerated method on special bench. Micro-sized dispersed industrial wastes were used as fillers: fly-ash from a power plant and spent filling material from a copper mining and processing plant. The results showed that the unfilled resin wear significantly decreases with increasing temperature, while the dependence on the temperature of the wear intensity at an impingement angle of 45° is linear inversely proportional, and at an angle of 90° non-linear. The decrease in wear intensity is probably due to an increase in elasticity (an increase in the fracture strain limit) because of heating. Solid particle erosion of the examined filled epoxy compounds is considerably higher than that of unfilled compounds at impingement angles of 90° and 45°. Filled compounds showed ambiguous dependences of intensity of wear from temperature (especially at an angle of attack 45°), probably, character of dependence is defined by a filler share and the structural features of the samples caused by distribution of particles of the filler. Intensity of wear of the considered compounds at impingement angles 90° and 45° has high direct correlation with density and the modulus of elasticity (i.e., increases with their increase), and low correlation with bending strength of the considered materials. The data set for determining the correlation between mechanical properties and wear included characteristics due to both compound filling and test temperature.

Keywords: solid particle erosion; epoxy resin; thermoset polymers; fly-ash; filled compound; elasticity modulus; bending strength

1. Introduction

Composite materials based on thermosetting resins (including epoxy resins) are widely used in different industries due to their corrosion resistance, high strength, and low weight. For example, they have recommended themselves in large-sized constructions of industrial exhaust ducts [1–4], operated at temperatures up to 100...120°C in systems with low content of dust particles in the diverted gases and, consequently, with a low level of abrasive impact on the inner surface of the exhaust duct.

Prospective is the use of structures from polymeric composite materials for gas exhaust ducts of metallurgical enterprises, but here in the composition of flue gases, which temperature can reach 180°C, there are particles of ash and metallurgical dust, causing abrasive wear of the inner surface of even steel elements of gas exhaust ducts [5]. Therefore, the study of resistance to gas abrasion of polymeric materials and composites is relevant and of practical importance.

Also actual is the problem of reducing the cost of composite materials used in the construction industry, this can be achieved by reducing the consumption of expensive polymeric binder, by filling it with various disperse additives. Besides decrease in consumption, filling of the binder may increase its mechanical characteristics (mainly stiffness)

 doi:10.20944/preprints202211.0377.v1

[6,7]. Various disperse additives can be used as fillers [6,8], at the same time an effective solution is the use of various fine-dispersed industrial waste (ashes, slags, etc.), because of their low cost, as well as the need for their utilization.

In the present work the object of research was unfilled and filled hot-curing epoxy binder on anhydride hardener. Fine-dispersed industrial wastes were used as fillers: fly ash from SDPP and spent filling material from a copper mining and processing plant. The subject of the research was solid particle erosion at room and elevated temperatures (up to 180°C).

Although polymeric binders are not structural materials themselves, but fiber-reinforced composites based on them (e.g., fiberglass plastics), we chose an unreinforced polymeric binder as an object of study because, as shown in [9–12], the resistance to gas abrasion of reinforced composites is lower than that of unreinforced polymeric binders used as a matrix. At the same time, the inner chemically resistant gel coat layer [13], which is a non-reinforced polymer binder in fact, is often performed in the gas exhaust ducts, which will be subjected to abrasion in the first place, playing the role of protective cover for the composite layer that takes mechanical load.

Analysis of references showed that the study of gas and hydro-abrasive wear of polymeric materials and composites on their basis is devoted to many works. In most of them, composites with polymer unfilled and filled matrices reinforced with different types of fibers are considered.

One of the well-known works on the study of solid particle erosion of polymer composites is the work [14], which lists the main factors influencing the intensity of erosion, studies composites with different types of reinforcing fibers and epoxy matrix. It is noted here that the wear of polymer composites is considerably higher than that of carbon steel at the same particle rate and that for ductile materials the maximum wear occurs at an angle of attack about 20°, and for brittle materials about 90°.

In work [8] a review of various factors influencing the intensity of solid particle erosion of glass-reinforced plastics with filled polymers matrix is given based on literature data. The influence of fillers (both artificial and natural) is considered. Also, the influence of experimental conditions (velocity, particle shape, impingement angle, etc.) is discussed. All the results have been obtained at room temperature. It is noted that, in some cases, filling the polymer matrix improves the resistance of the reinforced composite to solid particle erosion.

In [9] the resistance to solid particle erosion of carbon fiber-reinforced composites with unfilled and graphite powder-filled epoxy matrix was studied at room temperature (the filler content by weight was 2-6% of the weight of the whole composite, or 5-15% of the matrix weight). As a result, it was noted that the samples with unfilled matrix showed higher wear resistance than the filled ones at all impingement angles, the most intensive wear was observed at an angle of 45°.

In work [15] solid particle erosion of epoxy resins modified with hygrothermally decomposed polyester-urethane was studied at room temperature, corundum particles with sizes from 60 to 120 microns were used as abrasive. It is noted that the modified binders had a higher wear resistance compared to the unmodified ones.

In work [16] solid particle erosion of epoxy resin modified with synthetic oil was investigated at room temperature, quartz sand was used as abrasive, emitted at speeds from 6.5 to 9.5 m/s at different angles. As a result, it is noted that the modified binders had less brittleness and higher wear resistance compared to the non-modified ones.

In [17] the solid particle erosion of epoxy fiberglass plastic at room temperature was investigated including the filling of the matrix with fine-dispersed tungsten carbide powder. The conclusions noted that the filling improved the wear resistance of the fiberglass plastic, the microphotographs obtained on a scanning electron microscope showed more significant damage to the matrix and fibers in the composite with unfilled matrix, the most intense wear was observed at an impingement angle of 90°.

 doi:10.20944/preprints202211.0377.v1

In [18] at room temperature the solid particle erosion of epoxy resins filled with cenospheres was investigated, the result was that filling with cenospheres increased the wear resistance as compared to unfilled resin at all the impingement angles considered.

In [19] the solid particle erosion of glass fiber reinforced plastic with epoxy matrix filled with fly ash from Obra thermal power plant, Mirzapur, India was investigated at room temperature. As a result, it was observed that matrix filling reduced the wear rate of fiberglass compared to unfilled matrix. Hot-cured CY-205 epoxy resin with HY-951 anhydride hardener was used as the matrix.

In contrast to most of the above papers in [20] on the results of the study of solid particle erosion of carbon fiber reinforced plastic with epoxy unfilled and filled with nanoparticles montmorillonite matrix it was noted that the best wear resistance showed composite with unfilled epoxy matrix, that is in some cases fillers can reduce the wear resistance of polymer composites.

In all the aforementioned works the test methods were similar and corresponded to [21], but differed in several parameters, such as abrasive particle velocity, distance to the specimen, abrasive material shape, etc. All tests were conducted at room temperature.

It can be concluded from the above mentioned that the influence of polymer thermosetting binders filling on their wear resistance under gas-abrasive influence can be unambiguous. There are no results of research of solid particle erosion of unfilled hot-curing epoxy resins and filled with fly ash or slime of copper-mining plant at the increased temperatures up to 180°C (that exceeds the glass transition temperature of most epoxy binders) in the available literature sources. At the same time such data can be necessary for prediction of solid particle erosion during long-term operation of polymer composite structures of gas exhaust ducts of metallurgical enterprises.

2. Materials and Methods

2.1. Materials

To obtain the compounds in this work the following materials were used:

- KER 828 epoxy resin, with the following main characteristics: epoxy group content (EGC) 5308 mmol/kg, equivalent epoxy weight (EEW) 188.5 g/eq, viscosity at 25°C 12.7 Pa×s, HCl 116 mg/kg, total chlorine 1011 mg/kg. Manufacturer: KUMHO P&B Chemicals.

- Isomethyltetrahydrophthalic anhydride (IZOMTGFA) (hardener for epoxy resin) with the following main characteristics: viscosity at 25°C 63 Pa×s, anhydride content 42.4%, volatile fraction content 0.55%, free acid 0.1%. Manufacturer: ASAMBLY Chemicals company Ltd., Nanjing, China.

- Alkophen (epoxy curing booster) with the following main characteristics: viscosity at 25°C 150 Pa×s, molecular formula C15H27N3O, molecular weight 265, amine number 600 mg KOH/g. Manufacturer: JSC "Epital", Moscow, Russian Federation.

- Fly ash from SDPP (**Figure 1**, a): fraction 0.01-0.05 mm, specific surface 310 m^2/kg, bulk density 700 kg/m^3, the density of particles 1700 kg/m^3, modulus of elasticity of particles (approximately) 20000 MPa, CaO, MgO, SO_3, Na_2O, K_2O are in the composition.

- Backfill material was obtained from mineral processing waste of the copper-mining combine (**Figure 1**, b): it contains Quartz low (SiO_2) 20-30%, Aluminum Magnesium Hydroxide Silicate 5-15%, Magnesium Silicate (Serpentine) MgSiO3 5-10%, clay minerals (hydrated aluminosilicates) 20-40% and others. The material was pre-dried at 105°C and then crushed in a laboratory mill to a fraction of no more than 0.05 mm.

 doi:10.20944/preprints202211.0377.v1

a) b)

Figure 1. Appearance of the fillers used: a) Fly ash from the SDPP; b) Backfill material obtained from the mineral processing waste of the copper-mining plant

Compounds are shown in **Table 1**. The binders were mixed using a Stegler DG-360 mechanical disperser-homogenizer (China) with an M-shaped nozzle diameter of 17 mm and a nozzle rotation speed of 6000 rpm. After mixing, the binders were poured into silicone molds and placed in a laboratory oven for curing. The samples were cured at 110°C for 30 min. After initial curing, all samples were incubated at 150°C for 12 hours. Specimen preparation process showed in **Figure 2**.

a) b) c)

Figure 2. Specimen preparation process: a) mixing in a homogenizer; b) curing in a laboratory oven in a silicone mold; c) prepared specimens

Table 1. Types of binders investigated

№	Composition	Composition	Designation
1	Epoxy resin	Ker 828 52.5% + MTHPA 44.5% + Alkofen 3%	EP
2	0.25 w/w fly-ash filled epoxy resin	EP 50% + Fly-Ash 25%	EP-FA25
3	0.5 w/w fly-ash filled epoxy resin	EP 50% + Fly-Ash 50%	EP-FA50
4	0.33 w/w filling material filled epoxy resin	EP 67% + Filling material 33%	EP-FM33

All experimental specimens were made from a single binder mixture and five batches of specimens were made:

 doi:10.20944/preprints202211.0377.v1

- Batch №1 (EP1): immediately after mixing all the components (resin, hardener, and booster) the binder was poured into a silicone mold and placed in a laboratory oven for curing.

- Batch №2 (EP2): binder after mixing all components was kept for one hour at room temperature then poured into silicone molds and put into laboratory oven for curing.

- Batch №3 (EP-FA25): binder after mixing all components (including the filler) was maintained for an hour and a half at room temperature and then poured into a silicone mold and placed in a laboratory oven for curing.

- Batch №4 (EP-FA50): binder after mixing all components (including the filler) was maintained for two hours at room temperature and then poured into a silicone mold and placed in a laboratory oven for curing.

- Batch №5 (EP-FM33): the binder after mixing all components (including the filler) was maintained for two and a half hours at room temperature and then poured into a silicone mold and placed in a laboratory oven for curing.

From each batch, 90° and 45° test specimens were made (the same specimens were tested consecutively at different temperatures, but at the same angle of impingement).

2.2. Methods

As part of this work, in addition to solid particle erosion tests, three-point bending tests were carried out to determine the modulus of elasticity and bending strength, and the density of the samples was determined by hydrostatic weighing.

2.2.1. Solid particle erosion tests at elevated temperatures

To perform accelerated tests for gas abrasion resistance at elevated temperatures, an experimental bench was designed and manufactured (**Figure 3**).

The experimental bench includes the following main elements:

1. Thermally insulated lid with holder for the test specimen.
2. Metabo SSP 1000 sandblasting gun with a capacity of 300 l / min.
3. 1 kW tubular electric heating elements (THN) installed inside the enclosure in 2 pieces.
4. Case made of square steel bent-welded profile.
5. Socket for installing additional thermocouples.
6. Inspection hatch with heat-resistant glass.
7. Clamping holder to hold the sandblaster nozzle in place.

The bench is designed for accelerated solid particle erosion testing of plate samples of polymer and composite materials at room and elevated temperatures. The width of samples is 40...50 mm, height is 50...80 mm, thickness is 1...10 mm.

The abrasive impact is carried out with the Metabo SSP 1000 standard blast pistol with a 6 mm nozzle exit diameter, a capacity of 300 l/min (5 m^3/s) and an exit velocity of 115 m/s. The blast pistol can be set in two positions to test at angles of attack of 90^o and 45^o. The spent abrasive is poured into the lower part of the enclosure from where it is retrieved when the lower enclosure lid is opened.

The plate specimen is clamped in front of the nozzle of the sandblasting gun and abraded. The distance from the end of the nozzle to the specimen at an angle of attack of 90^o is 115 mm excluding the thickness of the specimen. The diameter of the blasted spot after one test is 27...30 mm.

Inside the case the air is heated by two heating elements of 1 kW each, the heating is controlled by the thermoregulator OVEN TRM500 with thermocouple DTPL054 00 100, installed on the upper cover of the case. Since in this design the compressed air is not heated, the abrasive material should be preheated to reduce the cooling of the specimen during high-temperature tests.

Compressed air is provided to the sandblaster by the NEXTTOOL compressor KMK-2300/100V with a capacity of 420 l/min, maximum pressure of 8 bar, volume of the receiver

Preprints (www.preprints.org) | NOT PEER-REVIEWED | Posted: 21 November 2022 doi:10.20944/preprints202211.0377.v1

of 100 l. The pressure in the receiver at the beginning of the test is 7.5 bar and at the end of the test is 6.0 bar.

Dimensions of plate specimens for wear tests were 60 x 40 mm, initial thickness of specimens was 4...8 mm. Dimensions of bend test specimens: length 70 mm, width 10 mm (± 1.0 mm), thickness 4 to 5 mm. Thickness of specimens was different as they were mechanically processed (grinded) to remove surface defects. Actual dimensions of the tested samples were measured with a caliper with an accuracy of 0.01 mm.

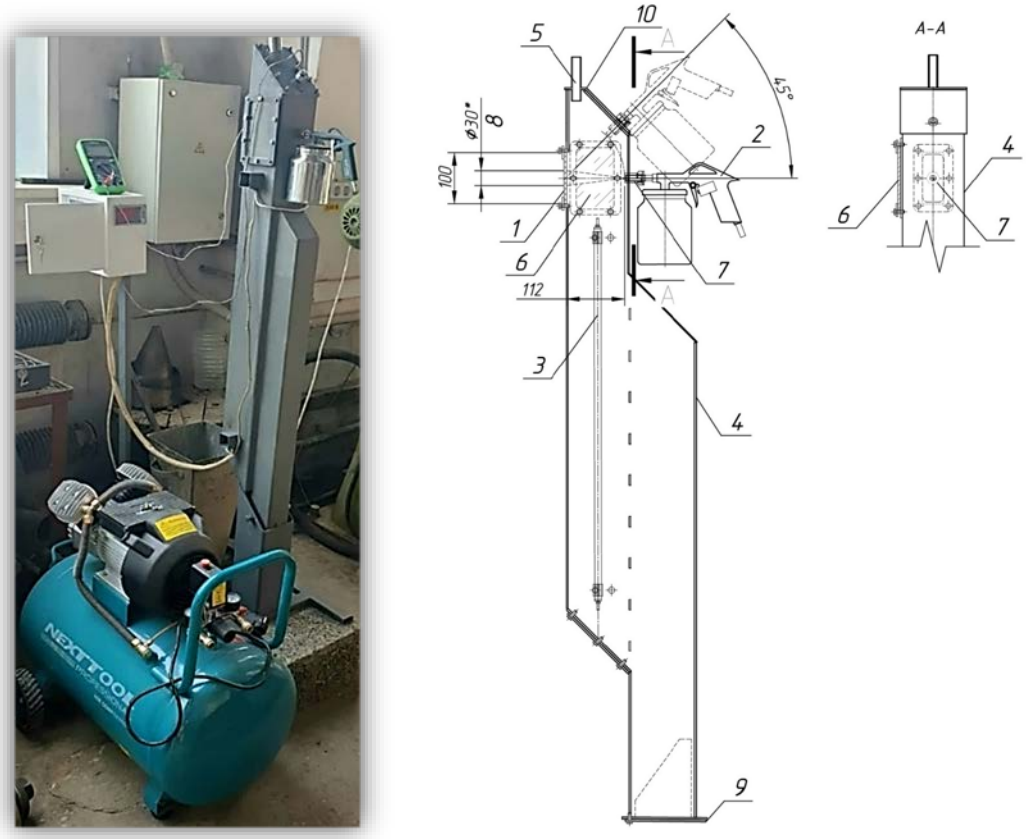

(a) (b)

Figure 3. Photo (a) and scheme (b) of the experimental stand for gas abrasion testing: 1 - insulated cover and holder for the test specimen; 2 - sandblasting gun Metabo SSP 1000; 3 - electric heater 1 kW (2 pcs.); 4 - steel case of the bench; 5 - socket for an additional thermocouple; 6 - inspection hatch with a heat-resistant glass; 7 - clamping holder for sandblaster nozzle; 8 - blasting spot; 9 - bottom lid; 10 - top lid.

Copper slag (**Figure 4**) with sharp angular-shaped grains of 0.125-0.63 mm in size, with a Mohs hardness of at least 6 and a grain density of 3.2-3.9 g/cm^3 is used as an abrasive.

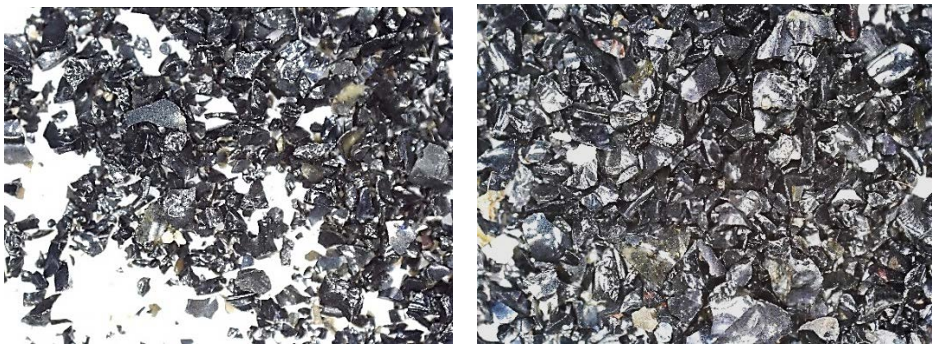

Figure 4. Photo on a scale of 10:1 of the used abrasive (Copper slag)

 doi:10.20944/preprints202211.0377.v1

Wear-resistance tests were carried out according to the following methodology:

- Preliminarily by hydrostatic weighing the density of samples was determined.
- A plate specimen was weighed with the accuracy of 0.001 g and set in the clamps of the experimental bench.
- 600 g of abrasive powder (Copper slag) were poured into the abrasive tank of the sandblaster.
- The sample was processed during the 1st minute.
- After processing, the volume was measured and weighed the spent abrasive, the average volume was 500 cm^3 at the weight of 975 - 1025 g (average bulk density of 1.95-2.05 g/cm^3).
- The sample was removed from the clamps of the stand and weighed again, the mass loss was determined.
- Through the loss of mass and density, the loss of volume of the material due to solid particle erosion was calculated.

The temperature of the specimen was monitored by an external thermocouple placed on the back of the specimen, which was not exposed to abrasion. Since the test procedure involves cooling the specimen through a stream of unheated air, the average between the pre-test and post-test temperatures was used as the temperature at which the wear was determined.

Because of the high intensity of abrasive effect, the wear of samples, tested by the offered technique will differ in a significant way from the wear of real constructions. However, the results of the tests can not only allow comparison of the wear resistance of the used materials but also with some assumptions to predict the resource in terms of solid particle erosion of the composite shell structures of the gas exhaust ducts.

2.2.2. Three-point bend tests at elevated temperature

Tests of three-point bending of binder samples at temperatures of 23°C and 100°C were conducted according to GOST R 56810-2015 [22] on the machine Tinius Olsen h100ku (Tinius Olsen GmbH, Goethestr. 7b, 86161 Augsburg, Germany) in a temperature chamber, which provides heating to 300°C. According to the passport data, the accuracy of load measuring of Tinius Olsen h100ku machine is ±0.5% in the range from 0.2 to 100% of the permissible load of the installed load cell (100 kN). The crosshead has a resolution of 0.001 mm with an accuracy of 0.01 mm. To eliminate the influence of machine compliance, displacement of the specimen center point under load was also controlled by a mechanical watch type indicator mounted under the specimen.

Specimens were cut from undamaged portions of the plates tested for wear and then tested over a span of 43 mm. The tests determined modulus of elasticity and bending strength.

Three-point bending tests determined the cured sample deformation modulus at temperatures of 23 and 100°C. The experimental values of elasticity modulus at the bending of the samples were determined at a 2 mm/min loading rate. The determination of the elasticity modulus was carried out under loading with two load steps.

When determining the elastic modulus in bending, the samples were preliminarily loaded with a concentrated force to the level of normal stresses of 5 MPa. Further, loading was carried out, and the determination of the elastic modulus was carried out at the range of normal stresses of 10 MPa.

The samples were preliminarily held at elevated temperatures until they were completely warmed up to the test temperature. The temperature during the tests was maintained by a thermostat and controlled by two thermocouples. One thermocouple measured the temperature on the surface of the bent specimen. The second thermocouple measured the temperature inside the control specimen, located next to the test specimen.

3. Results and Discussion

Preprints (www.preprints.org) | NOT PEER-REVIEWED | Posted: 21 November 2022 doi:10.20944/preprints202211.0377.v1

3.1. Solid particle erosion testing

The test results for all the samples from all the compounds examined are shown in the tables (**Table A. 1 – Table A. 24**) in Appendix A. A summary of the results for the tested resin types is given in **Table 2 – Table 5**, and the same data is shown graphically in **Figure 5**, **Figure 6**, **Figure 7**. The temperature columns in the tables show, outside parentheses, the temperature at the start of the test, and in parentheses, the average temperature during one test (which differs from the initial temperature due to cooling of the specimens during the test).

Statistical processing of the results was carried out in accordance with Section 4 and Annex 3 of standard GOST 14359-69* [23]. The values of normalized deviation distribution criterion in the small sample were determined in accordance with the number of tests for confidence probability 0.95. Values that were outside the confidence intervals (gross errors) were discarded (they are crossed out in the tables of Appendix A).

Table 2 Summary table of unfilled epoxy binder (EP) wear test results

Type of compound	Batch	Tests number	Variation coefficient (%)	Density (g/cm³)	Average VE (cm³)	Temperature (°C)	Impingement angle
EP	Ep1.1	8	20.13	1.167	**0.090**	23	90
		10	29.68		**0.035**	100 (96.5)	
		6	11.94		**0.073**	180 (165)	
	Ep1.2	8	21.11	1.167	**0.084**	23	
		10	23.75		**0.059**	100 (97)	
		6	5.29		**0.063**	180 (165)	
	Ep2.1	8	15.43	1.158	**0.217**	23	45
		6	10.23		**0.151**	100 (99)	
		6	14.3		**0.078**	180 (168)	
	Ep2.2	7	29.2	1.158	**0.271**	23	
		6	7.25		**0.189**	100 (101)	
		6	7.92		**0.083**	180 (173)	

Table 3 Summary table of a 25:75 (by weight) epoxy binder filled with fly ash (EP-FA25) wear test results

Type of compound	Batch	Tests number	Variation coefficient (%)	Density (g/cm³)	Average VE (cm³)	Temperature (°C)	Impingement angle
EP-FA25	EP-FA25	6	17.9	1.276	**0.096**	23	90
		6	23.84		**0.118**	100 (98)	
		6	29.03		**0.130**	180 (173)	
	EP-FA25	6	7.35	1.276	**0.493**	23	45
		6	5.27		**0.603**	100 (101)	
		6	3.28		**0.456**	180 (174)	

Table 4 Summary table of a 50:50 (by weight) epoxy binder filled with fly ash (EP-FA25) wear test results

Type of compound	Batch	Tests number	Variation coefficient (%)	Density (g/cm³)	Average VE (cm³)	Temperature (°C)	Impingement angle
EP-FA50	EP-FA50	6	15.31	1.415	**0.641**	23	90
		6	4.76		**0.446**	100 (100)	
		6	13.8		**0.640**	180 (172.5)	

Preprints (www.preprints.org) | NOT PEER-REVIEWED | Posted: 21 November 2022 doi:10.20944/preprints202211.0377.v1

	EP-FA50	6	2.74	1.415	**0.672**	23	45
		6	6.61		**0.686**	100 (99.5)	
		6	7.95		**0.883**	180 (175)	

Table 5 Summary table of wear test results of epoxy binder (EP-FM33) filled with spent filling material in 33:67 ratio (by weight)

Type of com-pound	Batch	Tests number	Variation coefficient (%)	Density (g/cm³)	Average VE (cm³)	Tempera-ture (°C)	Impinge-ment angle
EP-FM33	EP-FM33	13	29.15	1.330	**0.382**	23	90
		9	47.57		**0.110**	100 (96.5)	
		7	33.11		**0.179**	180 (173)	
	EP-FM33	13	33.74	1.330	**0.562**	23	45
		9	14.68		**0.397**	100 (96.7)	
		9	32.41		**0.183**	180 (166)	

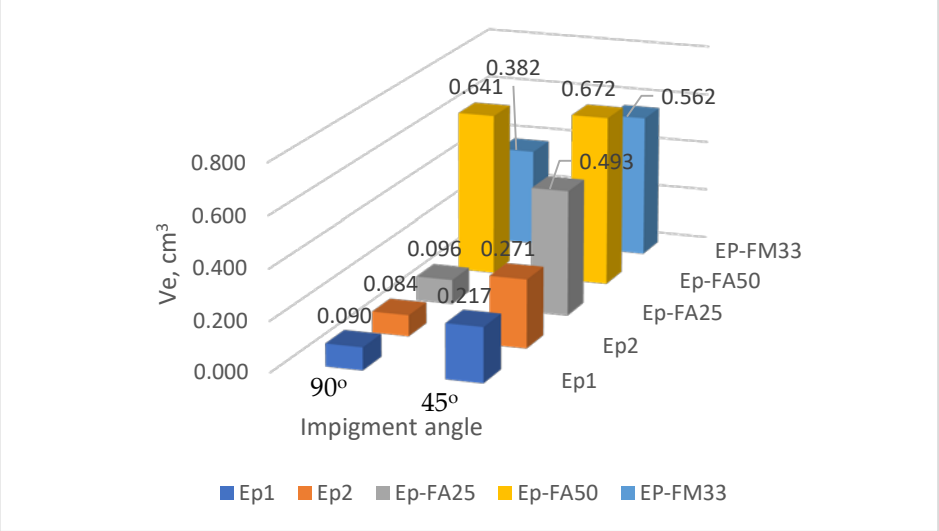

Figure 5. Compound wear at 23°C at 90° and 45° impingement angles

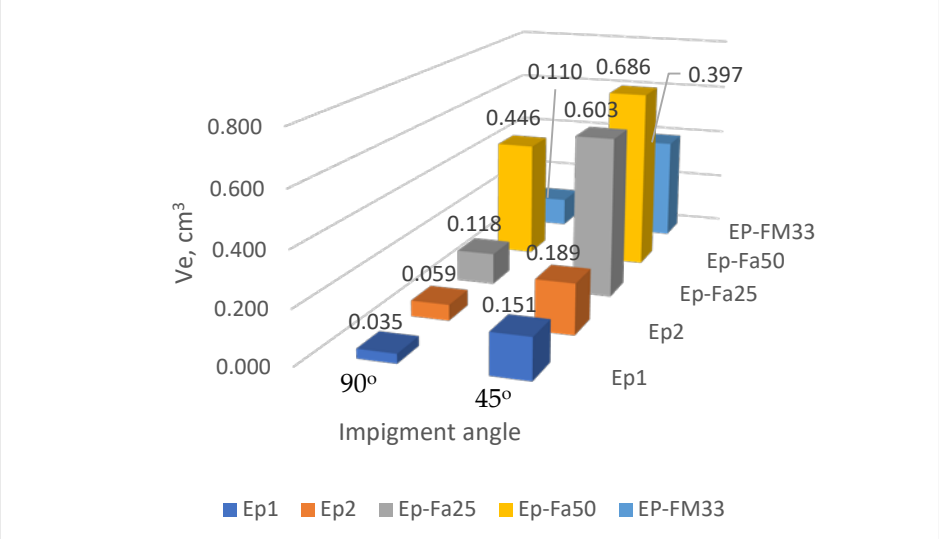

Figure 6. Compound wear at 100°C at 90° and 45° impingement angles

Preprints (www.preprints.org) | NOT PEER-REVIEWED | Posted: 21 November 2022 doi:10.20944/preprints202211.0377.v1

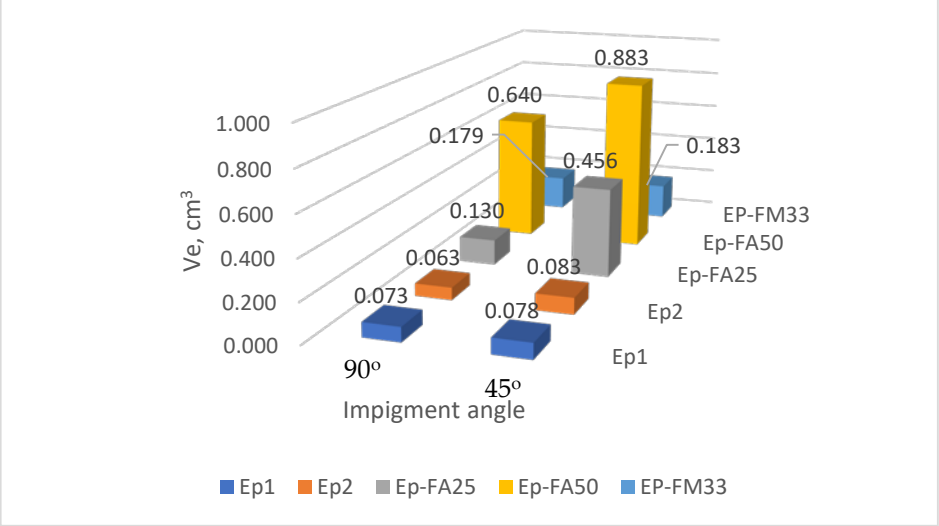

Figure 7. Compound wear at 180°C at 90° and 45° impingement angles

Figure 8 shows the temperature dependence of unfilled and filled com-pounds wear at an impingement angle of 90°. In all cases, the wear of filled compounds is significantly higher than that of unfilled ones. Maximum wear is observed for compound filled with fly-ash 50% (EP-FA50), at 23°C and 100°C it is about 7-7.5 times higher than unfilled compound wear, at temperature increase to 180°C the difference increases to 10 times.

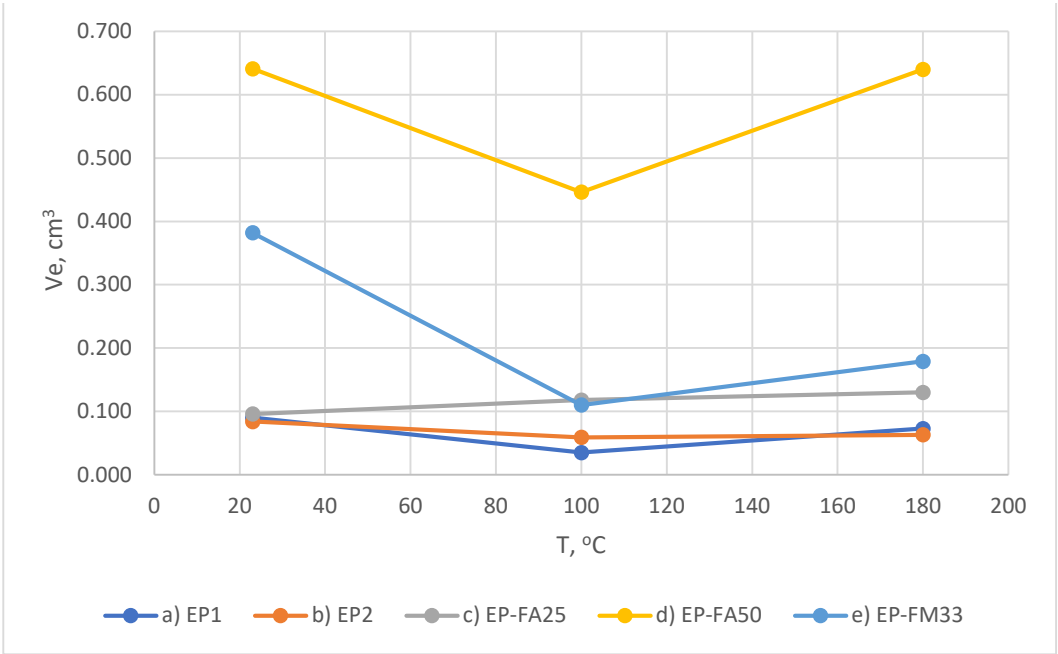

Figure 8. Dependence of wear of unfilled and filled compounds on temperature at an impingement angle of 90°

EP-FA25 compound at 23°C showed wear, practically coinciding with unfilled binders; further on, the wear rate increased linearly with increasing temperature, in contrast to all other compounds studied. Probably, this result can be explained by non-uniform distribution of filler particles over the specimen thickness, which is shown below in section 3.2. In other words, at the initial stage of erosion, mainly low-filled layers were subjected to wear, so the result is close to the unfilled compound.

The typical feature for the considered unfilled and filled compounds at an impingement angle of 90° (except EP-FA25) was a significant reduction of wear at 100°C, which does not exceed the glass transition temperature. For the unfilled compounds (batches Ep1.1, Ep1.2) the wear rate decreased in 1.5-2.5 times, for the filled EP-FA50 and EP-FM33

Preprints (www.preprints.org) | NOT PEER-REVIEWED | Posted: 21 November 2022 doi:10.20944/preprints202211.0377.v1

in 1.4 and 3.8 times respectively. This is associated with an increase in elasticity and ultimate fracture strain when heated, without a significant reduction in strength (which will also be shown in Section 3.2).

At 90° attack angle and 180°C (higher than glass transition temperature) all examined compounds showed higher wear than at 100°C, and in all cases (except EP-FM25) it did not exceed the wear rate at 23°C. At 180°C, the erosion pattern of the unfilled polymer surface changed and became significantly more uneven to the naked eye (**Figure 9**b).

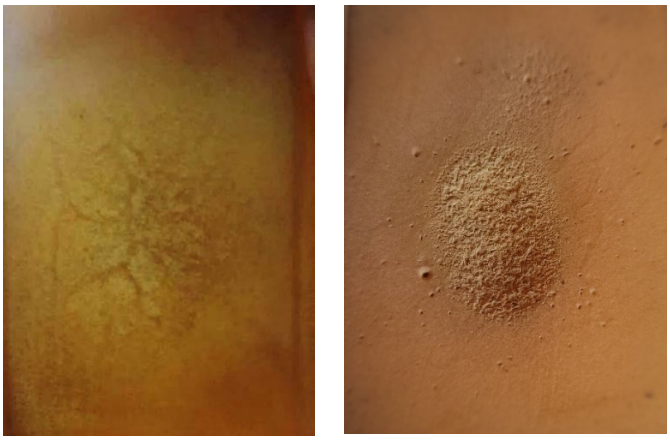

(a) (b)

Figure 9. Wear character of unfilled epoxy compound surface at an impingement angle of 90° at temperatures: a) up to 100°C; b) 180°C

Figure 10 shows the temperature dependence of wear of unfilled and filled compounds at an impingement angle of 45°, here as well as at an impingement angle of 90° in all cases the wear of filled compounds is significantly higher than that of unfilled ones. At 23°C compared to EP, the wear of the filled compounds is higher: 2.0 times for EP-FA25, 2.3 times for EP-FM33, 2.75 times for EP-FM50.

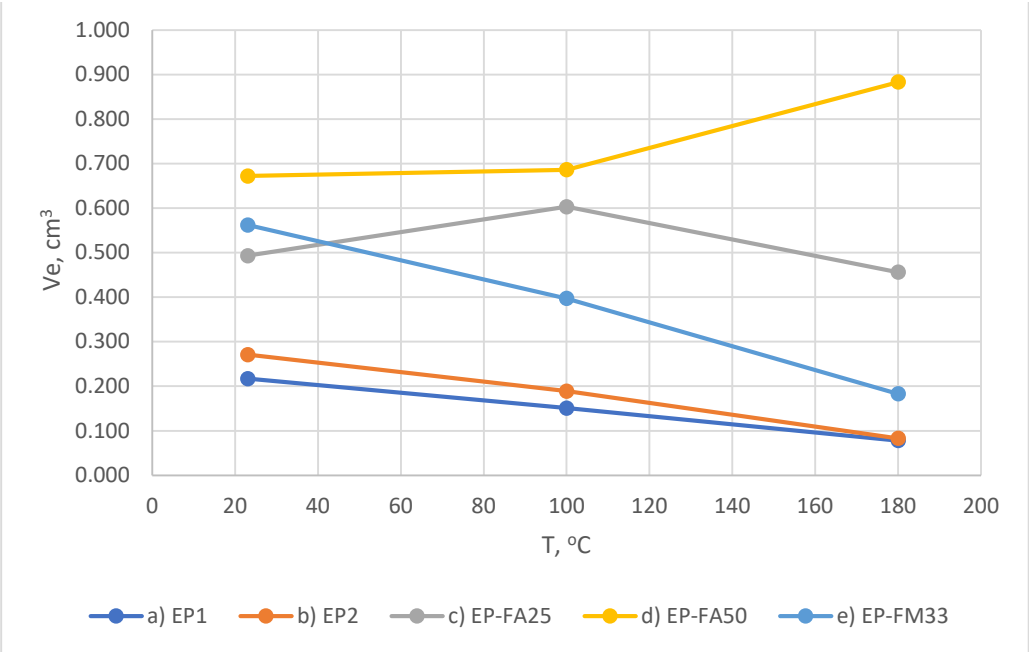

Figure 10. Dependence of wear of unfilled and filled compounds on temperature at an impingement angle of 45°

At impingement angle 45° and increasing temperature, the filled binders (as contrasted to impingement angle 90°) showed a different trend in wear rate under the same conditions. The maximum-filled EP-FA50 compound showed about the same wear rate at 23°C and 100°C, and at 180°C the wear rate increased by 30%. Compound EP-FA25 with

 doi:10.20944/preprints202211.0377.v1

temperature increase to 100°C showed the increase of wear degree by 20%, and with temperature increase to 180°C there was the decrease of wear degree by about 30%. Compound EP-FM33 (like the unfilled EP compound) showed a linear decrease in wear rate with increasing temperature.

The surface erosion pattern of the unfilled and filled sample at an impingement angle of 45° is shown in **Figure 11**.

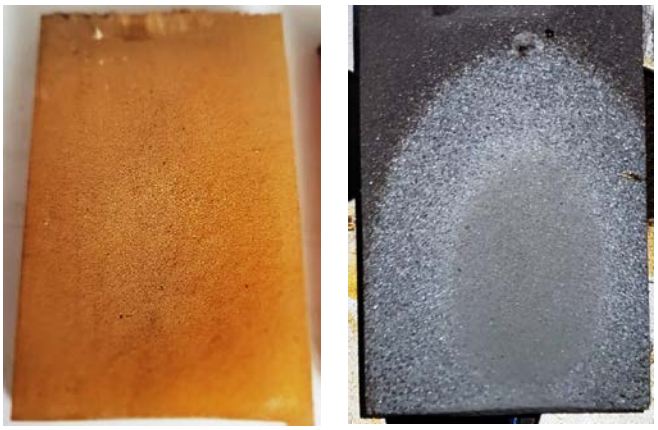

(a) (b)

Figure 11. Surface erosion character of unfilled (a) and filled (b) samples at an impingement angle of 45°

The various character of wear dependences on temperature for filled compounds, presumably, can be explained by structural features of samples, caused by properties of the filler, its percentage and distribution on the thickness of the sample. In the future, if it is necessary to clarify this question, it will be necessary to investigate wear at a smaller temperature step and, probably, to use modeling of the structure of hardened filled compounds and the impact of abrasive particles on them.

The most clearly seen dependences of wear on temperature (at impingement angle 90° and 45°) are observed for unfilled epoxy binder (batches EP1, EP2), for clarity they are shown separately in **Figure 12**. At 45° a clearly visible linear inversely proportional dependence of wear degree on temperature is observed. At 100° C the wear rate as compared to 23°C decreased by 1.4 times (for both batches of the binder), and at 180°C by 2.8-3.2 times.

At angle 90° the temperature dependence of wear rate on the temperature is nonlinear: when heated from 23°C to 100°C degree of wear decreases, then when heated to 180°C again slightly increases, but remains lower than at 23°C. At 180°C the degree of wear of unfilled samples at impingement angle of 90° and 45° is almost the same.

According to the work [14] the maximum intensity of solid particle erosion at impingement angle of 90° is typical for brittle materials, and at angle of 20° for ductile materials, i.e., with decrease of brittleness of material the degree of wear should increase at attempting impingement angle to 90°. The material, at which the maximum degree of wear is observed at 45° is called semi-ductile. In our case such simplified definition is not quite correct, because, as the experiments showed, with increasing of temperature from 23°C to 180° the difference of wear intensity between angles of attack 45° and 90° decreases, i.e., the brittleness contribution to the wear should increase and the ductility contribution should decrease, which is not appropriate for the unfilled epoxy binder, because its brittleness decreases, and ductility increases with heating.

 doi:10.20944/preprints202211.0377.v1

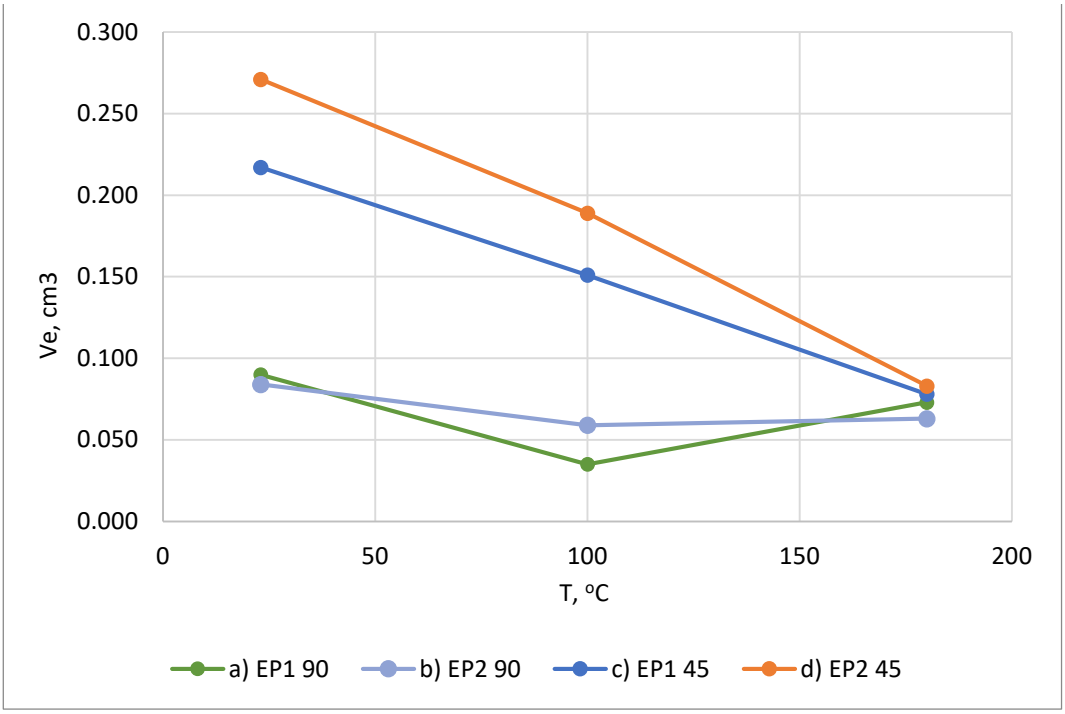

Figure 12. Dependence of wear of unfilled epoxy resin on temperature at an impingement angle of 90° and 45°

3.2. Three-point bending test

Determination of mechanical characteristics was carried out to estimate their correlation with the wear rate and to obtain data that can be used in the future in the design of composite structures.

Three-point bending tests to determine elastic modulus and bending strength were performed on beam specimens cut from plates that are previously tested for solid particle erosion, and the surface of the specimens was machined with an abrasive disk.

The unfilled epoxy binder specimens were divided into two groups, one group was tested at 23°C and the other at 100°C, according to the method described in Section 2.

After the wear tests it was able to produce a small number of filled bar samples of EP-FA50 and EP-FA25 binders, so they were not divided into groups and tested only at 23°C.

The bending test results for all specimens are shown in Appendix B, and the summary results for the different specimen types are shown in **Table 6**.

When tested at 100°C, the maximum deflection of the specimens was limited to 7 mm, but not all specimens were able to be broken due to the increase in elasticity (ultimate fracture strain) because of heating. Since the glass transition temperature was not reached, the specimens remained stiff enough to determine the modulus of elasticity in the stress range of 5-10 MPa.

The modulus of elasticity at 100°C decreased by 18% compared to the temperature of 23°C. The level of ultimate stresses in the specimens which broke down was slightly higher than the ultimate stresses in the specimens tested at 23°C. After testing and cooling, the unbroken specimens kept their deformed state at room temperature and recovered their original straight shape after heating to glass transition temperature. A test specimen that did not fracture is shown in **Figure 13**.

Preprints (www.preprints.org) | NOT PEER-REVIEWED | Posted: 21 November 2022 doi:10.20944/preprints202211.0377.v1

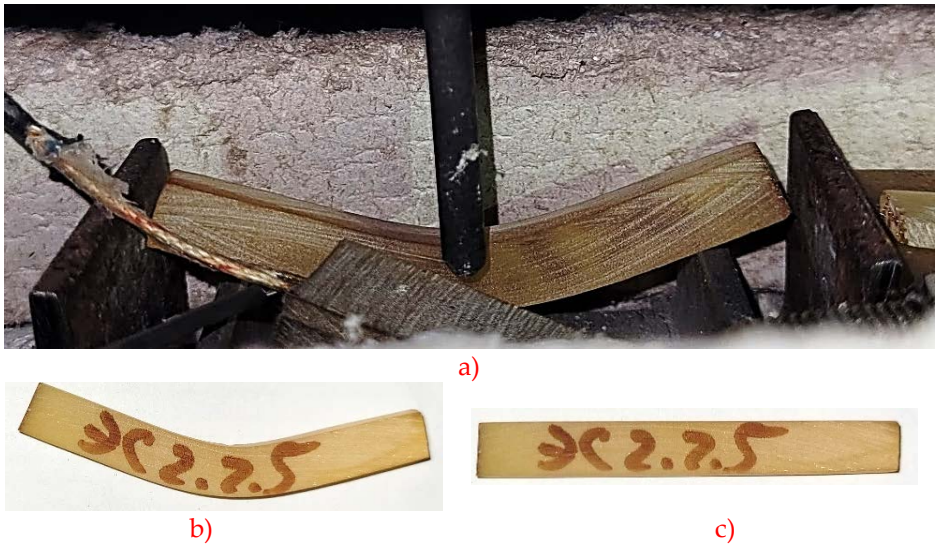

a)

b) c)

Figure 13. Photo of unfilled epoxy binder sample: a) during bending tests at 100°C; b) after removal of load and cooling in deformed (frozen) state; c) after heating to glass transition temperature and return to the original shape

The average values of elastic modulus and flexural strength of the filled compounds (EP-FA25, EP-FM33, EP-FA50) at 23°C are shown in **Table 6**. The results show a significant increase in modulus of elasticity when compared to the unfilled compounds (1.42 times for EP-FA25, 1.69 times for EP-FM33, 2.35 times for EP-FA50), with a smaller increase in strength (1.03 times for EP-FA25, 1.2 times for EP-FM33 and 1.14 times for EP-FA50).

Figure 14 shows enlarged cross sections of EP-FA25 (a) and EP-FA50 (b). The photo shows that the sample filled at 50% by weight has a more homogeneous structure (the filler is evenly distributed across the cross-section). The sample filled at 25% by weight has the largest particles of filler partially sedimented during the curing at high temperature and the liquefaction of epoxy resin. Despite this, all filled samples showed acceptable statistical variation in mechanical properties. **Figure 15** shows the experimental dependence of the modulus of elasticity of unfilled and filled compounds on their density.

a) b)

Figure 14. Photo of cross-sections of filled specimens: a) EP-FA25; b) EP-FA50

The correlation of wear values at impingement angle of 90o and 45o with elasticity modulus, strength and density of the examined specimens was evaluated using Microsoft Excel package.

The correlation coefficient between the sets of values X and Y is determined by the formula

$$Correl(X,Y) = \frac{\Sigma(x-\overline{x})(y-\overline{y})}{\sqrt{\Sigma(x-\overline{x})^2\,\Sigma(y-\overline{y})^2}},$$

Preprints (www.preprints.org) | NOT PEER-REVIEWED | Posted: 21 November 2022 doi:10.20944/preprints202211.0377.v1

if the correlation coefficient is close to 1 or -1, then there is a significant direct or inverse correlation between sets of values. The results of determining the correlation coefficient are presented in **Table 7**.

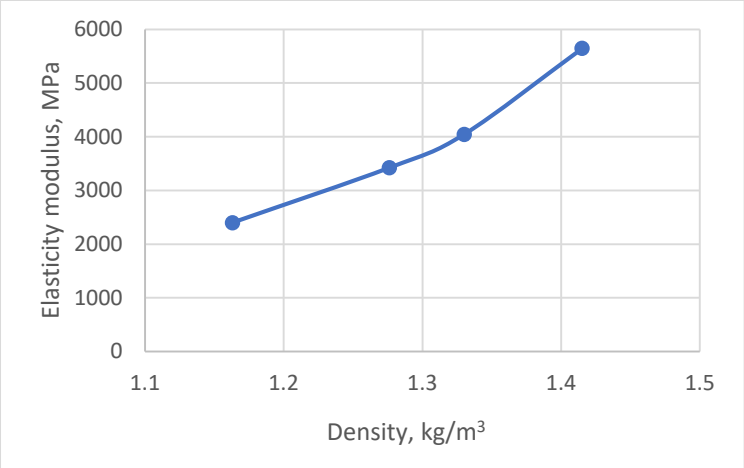

Figure 15. Dependence of elastic modulus on compound density

Table 6 Summary table of bend and wear test results

Type of compound	Temperature (°C)	Elastic Modulus (MPa)	Strength (MPa)	Average Erosion 90° (cm³)	Average Erosion 45° (cm³)	Density (g/cm³)	Modulus Variation Coefficient (%)	Strength Variation Coefficient (%)	Erosion 90° Variation Coefficient (%)	Erosion 45° Variation Coefficient (%)
EP	23	2398	60.7	0.087	0.244	1.163	12.9	36.6	20.62	22.32
EP	100	1970	71	0.047	0.170	1.163	28.1	11.0	26.18	8.74
EP-FA25	23	3421	62.4	0.096	0.493	1.276	11.4	27.2	17.9	7.35
EP-FA50	23	5645	69	0.641	0.672	1.415	8.1	8.6	15.31	2.74
EP-FM33	23	4045	73	0.382	0.562	1.33	17.1	19.5	29.15	33.74

Table 7 Correlation coefficients between physical and mechanical parameters and wear at different impingement angles

Parameters	Modulus of elasticity / erosion 90°	Modulus of elasticity / erosion 45°	Strength / erosion 90°	Strength / erosion 45°	Density / erosion 90°	Density / erosion 45°
Correlation coefficient	0.949	0.965	0.365	0.044	0.900	0.988

The results show that wear at impingement angles of 90° and 45° has a high direct correlation with the modulus of elasticity and density, and weak correlation with the flexural strength of the materials considered. In this case, the data set for determining the correlation included mechanical characteristics due to both the compound filling and the test temperature.

4. Conclusion

In general, the following conclusions can be made according to the results of the experimental studies:

1. At temperatures from 23°C to 100°C solid particle erosion rate of unfilled hot curing epoxy binder (EP) at an impingement angle of 45° is significantly higher than at an

 doi:10.20944/preprints202211.0377.v1

impingement angle of 90°. When the temperature is raised to 180°C the wear rates are nearly identical.

2. Solid particle erosion of unfilled epoxy binder (EP) decreases with temperature increase from 23°C to 180°C. At impingement angle 45° the dependence is clearly linear, at impingement angle 90° the dependence is non-linear: the wear intensity significantly decreases when heating from 23°C to 100°C, and at further heating to 180°C again slightly increases, but remains lower than at 23oC. The decrease in the wear rate is probably due to the increase in the fracture strain limit because of heating.

3. The solid particle erosion of considered filled epoxy compounds (EP-FA25, EP-FA50, EP-FM33) is significantly higher than unfilled epoxy compounds (EP) at 90° and 45°. For instance, the wear of EP-FA50 at impingement angle of 90° at temperatures of 23°C and 100°C is 7-7.5 times higher than EP, the difference increases by up to 10 times when the temperature goes up to 180°C. The filled compounds have shown differently directed dependence of wear rate on temperature (especially at impingement angle 45°), probably, character of dependence is defined by a level of filling and structural features of samples.

The wear intensity of the considered compounds at the impingement angles 90° and 45° has a high direct correlation with the density and the modulus of elasticity (i.e., increases with their increase), and weak correlation with the bending strength.

The obtained data on solid particle erosion of polymeric unfilled and filled epoxy compounds, for example, can be used to estimation of gas abrasion wear of composite shell structures of gas exhaust ducts during their service life. It should be noted that the used methodology of the solid particle erosion tests is accelerated, and the speed of the particles is much higher than in real operation conditions, that is why in order to use the obtained data for predicting the wear of real structures it is necessary to work out a methodology of extrapolation of the experimental data for the with a lower speed of solid particles.

Based on the obtained results the following practical conclusions can be made:

- it is reasonable to use filled compounds in the load bearing layers of structures for increasing their rigidity, and unfilled ones in the inner protective gel coat layers which are directly exposed to abrasive action.

- The unfilled epoxy binder considerably increases its resistance to gas abrasion when heated up to 100°C in comparison with the room temperature.

- At 180°C, higher than the glass transition temperature the gas abrasion resistance of the examined epoxy binder also increased, but at impingement angle 90° the character of surface erosion changed, it became significantly more eroded.

Also, for practical application of the considered materials in the conditions of combined gas-abrasive influence and increased temperature in the future it is necessary to investigate the influence of such factors, as chemically aggressive substances, thermal aging, stress state, etc., on the resistance to solid particle erosion.

Funding: The research was performed within the Ministry of Science and Higher Education of the Russian Federation state assignment FENU-2020-0019

References

1. Graham J. APPLICATION OF GLASS REINFORCED PLASTIC IN A RECOVERY BOILER CHIMNEY. // Can Pulp Pap Assoc CPPA Tech Sect Proc. 1973.
2. Pritchard B.N. Industrial chimneys: A review of the current state of the art // Proceedings of the Institution of Civil Engineers: Structures and Buildings. 1996.
3. Bochicchio V.A. FRP chimney liners for power plant flue gas desulfurization - A chimney supplier's perspective // NACE - International Corrosion Conference Series. 2011.
4. Astashkin V.M., Mishnev M. v. On the Development of the Manufacturing Technology of Fiberglass Cylindrical Shells of Gas Exhaust Trunks by Buildup Winding // Procedia Engineering. 2016. Vol. 150.

5. D. S. Zhu et al. Gas-Solid Erosion Study of Elbow Pipe based on Erosion Dynamic Grid Technology // Journal of Applied Fluid Mechanics. 2022. Vol. 15, № 6.
6. Hanafi Ismail, S. M. Sapuan, Rushdan Ahmad Ilyas. Mineral-Filled Polymer Composites Handbook, Two-Volume Set. CRC Press, 2022. 1–508 p.
7. Rajak D. et al. Fiber-Reinforced Polymer Composites: Manufacturing, Properties, and Applications // Polymers (Basel). 2019. Vol. 11, № 10. P. 1667.
8. Shahapurkar K. et al. Factors affecting the solid particle erosion of environment pollutant and natural particulate filled polymer composites—A review // Polymers and Polymer Composites. 2021. Vol. 29, № 9.
9. Sudarshan Rao K., Varadarajan Y.S., Rajendra N. Erosive Wear Behaviour of Carbon Fiber-reinforced Epoxy Composite // Materials Today: Proceedings. 2015. Vol. 2, № 4–5.
10. Tewari U.S. et al. Solid particle erosion of carbon fibre- and glass fibre-epoxy composites // Compos Sci Technol. 2003. Vol. 63, № 3–4.
11. Antonov M. et al. The effect of fine erodent retained on the surface during erosion of metals, ceramics, plastic, rubber and hardmetal // Wear. 2016. Vol. 354–355.
12. Mishnev M. V., Korolev A. S. Solid particle erosion wear of thermosetting polymers and composites at room and elevated temperatures: an experimental study // Construction of Unique Buildings and Structures. 2021. Vol. 5, № 98.
13. V.M. Astashkin, V.S. Zholudov. CHIMNEYS AND ELEMENTS OF GAS-ESCAPE PATHS MADE OF POLYMER COMPOSITES, 2011. 1–155 p.
14. Pool K.V., Dharan C.K.H., Finnie I. Erosive wear of composite materials // Wear. 1986. Vol. 107, № 1. P. 1–12.
15. Barkoula N.M., Gremmels J., Karger-Kocsis J. Dependence of solid particle erosion on the cross-link density in an epoxy resin modified by hygrothermally decomposed polyurethane // Wear. 2001. Vol. 247, № 1.
16. Atia A. M., Ali W. Y. Particle Erosion of Epoxy Resin // ournal of Multidisciplinary Engineering Science and Technology (JM. 2016. Vol. 3, № 5. P. 4780–4784.
17. Mohan N., Mahesha C.R., Rajaprakash B.M. Erosive wear behaviour of WC filled glass epoxy composites // Procedia Engineering. 2013. Vol. 68.
18. Shahapurkar K. et al. Effect of cenosphere filler surface treatment on the erosion behavior of epoxy matrix syntactic foams // Polym Compos. 2019. Vol. 40, № 6.
19. Srivastava V.K., Pawar A.G. Solid particle erosion of glass fibre reinforced flyash filled epoxy resin composites // Compos Sci Technol. 2006. Vol. 66, № 15.
20. Ismail M. et al. Parametric appraisal of erosion behaviour of organo-modified montmorillonite-filled epoxy hybrid composites by Taguchi approach // Journal of Reinforced Plastics and Composites. 2013. Vol. 32, № 21.
21. ASTM G76 - 13. Standard Test Method for Conducting Erosion Tests by Solid Particle Impingement Using Gas Jets. ASTM International, 2013.
22. National standard GOST RF 56810-2015 Polymer composites. Test method for flexural flat samples. 2017.
23. GOST 14359-69* Plastics. Testing methods. General requirements of the methods of mechanical testing.

Preprints (www.preprints.org) | NOT PEER-REVIEWED | Posted: 21 November 2022 doi:10.20944/preprints202211.0377.v1

Appendix A

Table A. 1 Wear of unfilled epoxy binder (EP) at 23° C at an impingement angle of 90°

Type of compound	Batch	Test Specimen No	Mass change Δm (g)	Density (g/cm³)	Volume of erosion VE (cm³)	Average VE (cm³)	Variation coefficient %
EP	Ep1.1	1	0.146	1.167	0.125	**0.090**	**20.13**
		2	0.120	1.167	0.103		
		3	0.108	1.167	0.093		
		4	0.084	1.167	0.072		
	Ep1.2	1	0.108	1.167	0.093		
		2	0.098	1.167	0.084		
		3	0.092	1.167	0.079		
		4	0.082	1.167	0.070		
	Ep2.1	1	0.074	1.158	0.064	**0.084**	**21.11**
		2	0.092	1.158	0.079		
		3	0.118	1.158	0.102		
		4	0.132	1.158	0.114		
	Ep2.2	1	0.098	1.158	0.085		
		2	0.070	1.158	0.060		
		3	0.098	1.158	0.085		
		4	0.074	1.158	0.064		

Table A. 2 Wear of unfilled epoxy binder (EP) at 23° C at an impingement angle of 45°

Type of compound	Batch	Test Specimen No	Mass change Δm (g)	Density (g/cm³)	Volume of erosion VE (cm³)	Average VE (cm³)	Variation coefficient %
EP	Ep1.3	1	0.176	1.167	0.151	**0.217**	**15.43**
		2	0.228	1.167	0.195		
		3	0.232	1.167	0.199		
		4	0.266	1.167	0.228		
	Ep1.4	1	0.268	1.167	0.230		
		2	0.282	1.167	0.242		
		3	0.284	1.167	0.243		
		4	0.292	1.167	0.250		
	Ep2.3	1	0.344	1.158	0.297	~~**0.300**~~ **0.271**	**29.20**
		2	0.330	1.158	0.285		
		3	0.332	1.158	0.287		
		4	0.344	1.158	0.297		
	Ep2.4	1	0.262	1.158	0.226		
		2	0.286	1.158	0.247		
		3	~~0.588~~	~~1.158~~	~~0.508~~		
		4	0.296	1.158	0.256		

Preprints (www.preprints.org) | NOT PEER-REVIEWED | Posted: 21 November 2022 doi:10.20944/preprints202211.0377.v1

Table A. 3 Wear of unfilled epoxy binder (EP) at 100° C at an impingement angle of 90°

Type of compound	Batch	Test Specimen No	Mass change Δm (g)	Density (g/cm³)	Volume of erosion VE (cm³)	Average VE (cm³)	Variation coefficient %
EP	Ep1.1	1	0.026	1.167	0.022	**0.035**	**29.68**
		2	0.054	1.167	0.046		
		3	0.050	1.167	0.043		
	Ep1.2	1	0.022	1.167	0.019		
		2	0.042	1.167	0.036		
		3	0.030	1.167	0.026		
	Ep1.9	1	0.050	1.167	0.043		
		2	0.056	1.167	0.048		
		3	0.038	1.167	0.033		
		4	0.036	1.167	0.031		
	Ep2.1	1	0.098	1.158	0.085	**0.059**	**23.75**
		2	0.082	1.158	0.071		
		3	0.072	1.158	0.062		
	Ep2.2	1	0.080	1.158	0.069		
		2	0.062	1.158	0.054		
		3	0.060	1.158	0.052		
	Ep2.9	1	0.056	1.158	0.048		
		2	0.060	1.158	0.052		
		3	0.078	1.158	0.067		
		4	0.040	1.158	0.035		

Table A. 4 Wear of unfilled epoxy binder (EP) at 100° C at an impingement angle of 45°

Type of compound	Batch	Test Specimen No	Mass change Δm (g)	Density (g/cm³)	Volume of erosion VE (cm³)	Average VE (cm³)	Variation coefficient %
EP	Ep1.3	1	0.208	1.167	0.178	**0.151**	**10.23**
		2	0.186	1.167	0.159		
		3	0.166	1.167	0.142		
	Ep1.4	1	0.158	1.167	0.135		
		2	0.172	1.167	0.147		
		3	0.168	1.167	0.144		
	Ep2.3	1	0.206	1.158	0.178	**0.189**	**7.25**
		2	0.246	1.158	0.212		
		3	0.204	1.158	0.176		
	Ep2.4	1	0.210	1.158	0.181		
		2	0.226	1.158	0.195		
		3	0.222	1.158	0.192		

Table A. 5 Wear of unfilled epoxy binder (EP) at 180° C at an impingement angle of 90°

Type of compound	Batch	Test Specimen No	Mass change Δm (g)	Density (g/cm³)	Volume of erosion VE (cm³)	Average VE (cm³)	Variation coefficient %
EP	Ep1.1	1	0.080	1.167	0.069	**0.073**	**11.94**
		2	0.090	1.167	0.077		
		3	0.076	1.167	0.065		
	Ep1.2	1	0.076	1.167	0.065		
		2	0.090	1.167	0.077		
		3	0.102	1.167	0.087		

Preprints (www.preprints.org) | NOT PEER-REVIEWED | Posted: 21 November 2022 doi:10.20944/preprints202211.0377.v1

Ep2.1	1	0.077	1.158	0.066	**0.063**	**5.29**
	2	0.074	1.158	0.064		
	3	0.078	1.158	0.067		
Ep2.2	1	0.074	1.158	0.064		
	2	0.068	1.158	0.059		
	3	0.070	1.158	0.060		

Table A. 6 Wear of unfilled epoxy binder (EP) at 180°C at an impingement angle of 45°

Type of compound	Batch	Test Specimen No	Mass change Δm (g)	Density (g/cm³)	Volume of erosion VE (cm³)	Average VE (cm³)	Variation coefficient %
EP	Ep1.3	1	0.084	1.167	0.072	**0.078**	**14.30**
		2	0.096	1.167	0.082		
		3	0.090	1.167	0.077		
	Ep1.4	1	0.104	1.167	0.089		
		2	0.070	1.167	0.060		
		3	0.104	1.167	0.089		
	Ep2.3	1	0.102	1.158	0.088	**0.083**	**7.92**
		2	0.104	1.158	0.090		
		3	0.104	1.158	0.090		
	Ep2.4	1	0.088	1.158	0.076		
		2	0.088	1.158	0.076		
		3	0.094	1.158	0.081		

Table A. 7 Wear of filled epoxy binder (EP-FA25) at 23°C at an impingement angle of 90°

Type of compound	Batch	Test Specimen No	Mass change Δm (g)	Density (g/cm³)	Volume of erosion VE (cm³)	Average VE (cm³)	Variation coefficient %
EP-FA25	EP-FA25.1	1	0.114	1.276	0.089	**0.096**	**17.90**
		2	0.140	1.276	0.110		
		3	0.120	1.276	0.094		
	EP-FA25.2	1	0.084	1.276	0.066		
		2	0.130	1.276	0.102		
		3	0.144	1.276	0.113		

Table A. 8 Wear of filled epoxy binder (EP-FA25) at 23°C at an impingement angle of 45°

Type of compound	Batch	Test Specimen No	Mass change Δm (g)	Density (g/cm³)	Volume of erosion VE (cm³)	Average VE (cm³)	Variation coefficient %
EP-FA25	EP-FA25.3	1	0.670	1.276	0.525	**0.493**	**7.35**
		2	0.676	1.276	0.530		
		3	0.560	1.276	0.439		
	EP-FA25.4	1	0.652	1.276	0.511		
		2	0.630	1.276	0.494		
		3	0.590	1.276	0.462		

Preprints (www.preprints.org) | NOT PEER-REVIEWED | Posted: 21 November 2022 doi:10.20944/preprints202211.0377.v1

Table A. 9 Wear of filled epoxy binder (EP-FA25) at 100°C at an impingement angle of 90°

Type of compound	Batch	Test Specimen No	Mass change Δm (g)	Density (g/cm³)	Volume of erosion VE (cm³)	Average VE (cm³)	Variation coefficient %
EP-FA25	EP-FA25.1	1	0.092	1.276	0.072	**0.118**	**23.84**
		2	0.196	1.276	0.154		
		3	0.176	1.276	0.138		
	EP-FA25.2	1	0.160	1.276	0.125		
		2	0.140	1.276	0.110		
		3	0.140	1.276	0.110		

Table A. 10 Wear of filled epoxy binder (EP-FA25) at 100°C at an impingement angle of 45°

Type of compound	Batch	Test Specimen No	Mass change Δm (g)	Density (g/cm³)	Volume of erosion VE (cm³)	Average VE (cm³)	Variation coefficient %
EP-FA25	EP-FA25.3	1	0.760	1.276	0.596	**0.603**	**5.27**
		2	0.744	1.276	0.583		
		3	0.708	1.276	0.555		
	EP-FA25.4	1	0.820	1.276	0.643		
		2	0.784	1.276	0.614		
		3	0.800	1.276	0.627		

Table A. 11 Wear of filled epoxy binder (EP-FA25) at 180°C at an impingement angle of 90°

Type of compound	Batch	Test Specimen No	Mass change Δm (g)	Density (g/cm³)	Volume of erosion VE (cm³)	Average VE (cm³)	Variation coefficient %
EP-FA25	EP-FA25.1	1	0.148	1.276	0.116	**0.130**	**29.03**
		2	0.192	1.276	0.150		
		3	0.240	1.276	0.188		
	EP-FA25.2	1	0.176	1.276	0.138		
		2	0.100	1.276	0.078		
		3	0.140	1.276	0.110		

Table A. 12 Wear of filled epoxy binder (EP-FA25) at 180°C at an impingement angle of 45°

Type of compound	Batch	Test Specimen No	Mass change Δm (g)	Density (g/cm³)	Volume of erosion VE (cm³)	Average VE (cm³)	Variation coefficient %
EP-FA25	EP-FA25.3	1	0.612	1.276	0.480	**0.456**	**3.28**
		2	0.572	1.276	0.448		
		3	0.560	1.276	0.439		
	EP-FA25.4	1	0.572	1.276	0.448		
		2	0.596	1.276	0.467		
		3	0.576	1.276	0.451		

Preprints (www.preprints.org) | NOT PEER-REVIEWED | Posted: 21 November 2022 doi:10.20944/preprints202211.0377.v1

Table A. 13 Wear of filled epoxy binder (EP-FA50) at 23°C at an impingement angle of 90°

Type of compound	Batch	Test Specimen No	Mass change Δm (g)	Density (g/cm³)	Volume of erosion VE (cm³)	Average VE (cm³)	Variation coefficient %
EP-FA50	EP-FA50.1	1	0.738	1.415	0.522	**0.641**	**15.31**
		2	0.844	1.415	0.596		
		3	0.908	1.415	0.642		
	EP-FA50.2	1	1.152	1.415	0.814		
		2	0.940	1.415	0.664		
		3	0.856	1.415	0.605		

Table A. 14 Wear of filled epoxy binder (EP-FA50) at 23°C at an impingement angle of 45°

Type of compound	Batch	Test Specimen No	Mass change Δm (g)	Density (g/cm³)	Volume of erosion VE (cm³)	Average VE (cm³)	Variation coefficient %
EP-FA50	EP-FA50.3	1	0.948	1.415	0.670	**0.672**	**2.74**
		2	0.912	1.415	0.645		
		3	0.980	1.415	0.693		
	EP-FA50.4	1	0.980	1.415	0.693		
		2	0.944	1.415	0.667		
		3	0.940	1.415	0.664		

Table A. 15 Wear of filled epoxy binder (EP-FA50) at 100°C at an impingement angle of 90°

Type of compound	Batch	Test Specimen No	Mass change Δm (g)	Density (g/cm³)	Volume of erosion VE (cm³)	Average VE (cm³)	Variation coefficient %
EP-FA50	EP-FA50.1	1	0.648	1.415	0.458	**0.446**	**4.76**
		2	0.656	1.415	0.464		
		3	0.632	1.415	0.447		
	EP-FA50.2	1	0.652	1.415	0.461		
		2	0.620	1.415	0.438		
		3	0.576	1.415	0.407		

Table A. 16 Wear of filled epoxy binder (EP-FA50) at 100°C at an impingement angle of 45°

Type of compound	Batch	Test Specimen No	Mass change Δm (g)	Density (g/cm³)	Volume of erosion VE (cm³)	Average VE (cm³)	Variation coefficient %
EP-FA50	EP-FA50.3	1	0.856	1.415	0.605	**0.686**	**6.61**
		2	0.964	1.415	0.681		
		3	0.996	1.415	0.704		
	EP-FA50.4	1	1.012	1.415	0.715		
		2	1.040	1.415	0.735		
		3	0.956	1.415	0.676		

 doi:10.20944/preprints202211.0377.v1

Table A. 17 Wear of filled epoxy binder (EP-FA50) at 180°C at an impingement angle of 90°

Type of compound	Batch	Test Specimen No	Mass change Δm (g)	Density (g/cm³)	Volume of erosion VE (cm³)	Average VE (cm³)	Variation coefficient %
EP-FA50	EP-FA50.1	1	0.864	1.415	0.611	**0.640**	**13.80**
		2	0.916	1.415	0.647		
		3	0.816	1.415	0.577		
	EP-FA50.2	1	0.840	1.415	0.594		
		2	1.152	1.415	0.814		
		3	0.848	1.415	0.599		

Table A. 18 Wear of filled epoxy binder (EP-FA50) at 180°C at an impingement angle of 45°

Type of compound	Batch	Test Specimen No	Mass change Δm (g)	Density (g/cm³)	Volume of erosion VE (cm³)	Average VE (cm³)	Variation coefficient %
EP-FA50	EP-FA50.3	1	1.164	1.415	0.823	**0.883**	**7.95**
		2	1.148	1.415	0.811		
		3	1.168	1.415	0.825		
	EP-FA50.4	1	1.336	1.415	0.944		
		2	1.364	1.415	0.964		
		3	1.316	1.415	0.930		

Table A. 19 Wear of filled epoxy binder (EP-FM50) at 23°C at an impingement angle of 90°

Type of compound	Batch	Test Specimen No	Mass change Δm (g)	Density (g/cm³)	Volume of erosion VE (cm³)	Average VE (cm³)	Variation coefficient %
EP-FM50	EP-FM50.1	1	0.656	1.33	0.493	**0.382**	**29.15**
		2	0.592	1.33	0.445		
		3	0.568	1.33	0.427		
		4	0.756	1.33	0.568		
		5	0.556	1.33	0.418		
	EP-FM50.2	1	0.484	1.33	0.364		
		2	0.424	1.33	0.319		
		3	0.340	1.33	0.256		
		4	0.332	1.33	0.250		
		5	0.284	1.33	0.214		
	EP-FM50.3	1	0.708	1.33	0.532		
		2	0.500	1.33	0.376		
		3	0.408	1.33	0.307		

 doi:10.20944/preprints202211.0377.v1

Table A. 20 Wear of filled epoxy binder (EP-FM50) at 23°C at an impingement angle of 45°

Type of compound	Batch	Test Specimen No	Mass change Δm (g)	Density (g/cm³)	Volume of erosion VE (cm³)	Average VE (cm³)	Variation coefficient %
EP-FM50	EP-FM50.4	1	0.472	1.33	0.355	**0.562**	**33.74**
		2	0.464	1.33	0.349		
		3	0.452	1.33	0.340		
		4	0.476	1.33	0.358		
		5	0.484	1.33	0.364		
	EP-FM50.5	1	1.028	1.33	0.773		
		2	1.044	1.33	0.785		
		3	0.796	1.33	0.598		
		4	0.832	1.33	0.626		
		5	0.764	1.33	0.574		
	EP-FM50.6	1	1.140	1.33	0.857		
		2	0.952	1.33	0.716		
		3	0.820	1.33	0.617		

Table A. 21 Wear of filled epoxy binder (EP-FM50) at 100°C at an impingement angle of 90°

Type of compound	Batch	Test Specimen No	Mass change Δm (g)	Density (g/cm³)	Volume of erosion VE (cm³)	Average VE (cm³)	Variation coefficient %
EP-FM50	EP-FM50.1	1	0.100	1.33	0.075	**0.127**	**47.57**
		2	0.088	1.33	0.066		
		3	0.352	1.33	0.265		
	EP-FM50.2	1	0.168	1.33	0.126		
		2	0.144	1.33	0.108		
		3	0.100	1.33	0.075		
	EP-FM50.3	1	0.200	1.33	0.150		
		2	0.180	1.33	0.135		
		3	0.188	1.33	0.141		

Table A. 22 Wear of filled epoxy binder (EP-FM50) at 100°C at an impingement angle of 45°

Type of compound	Batch	Test Specimen No	Mass change Δm (g)	Density (g/cm³)	Volume of erosion VE (cm³)	Average VE (cm³)	Variation coefficient %
EP-FM50	EP-FM50.4	1	0.448	1.33	0.337	**0.397**	**14.68**
		2	0.460	1.33	0.346		
		3	0.472	1.33	0.355		
	EP-FM50.5	1	0.556	1.33	0.418		
		2	0.532	1.33	0.400		
		3	0.468	1.33	0.352		
	EP-FM50.6	1	0.692	1.33	0.520		
		2	0.572	1.33	0.430		
		3	0.556	1.33	0.418		

Preprints (www.preprints.org) | NOT PEER-REVIEWED | Posted: 21 November 2022 doi:10.20944/preprints202211.0377.v1

Table A. 23 Wear of filled epoxy binder (EP-FM50) at 180°C at an impingement angle of 90°

Type of compound	Batch	Test Specimen No	Mass change Δm (g)	Density (g/cm³)	Volume of erosion VE (cm³)	Average VE (cm³)	Variation coefficient %
EP-FM50	EP-FM50.1	1	0.316	1.33	0.238		
		2	0.356	1.33	0.268		
		3	0.284	1.33	0.214		
	EP-FM50.2	1	0.200	1.33	0.150	**0.179**	**33.11**
		2	0.176	1.33	0.132		
		3	0.160	1.33	0.120		
	EP-FM50.3	1	0.176	1.33	0.132		

Table A. 24 Wear of filled epoxy binder (EP-FM50) at 180°C at an impingement angle of 45°

Type of compound	Batch	Test Specimen No	Mass change Δm (g)	Density (g/cm³)	Volume of erosion VE (cm³)	Average VE (cm³)	Variation coefficient %
EP-FM50	EP-FM50.4	1	0.152	1.33	0.114		
		2	0.140	1.33	0.105		
		3	0.136	1.33	0.102		
	EP-FM50.5	1	0.252	1.33	0.189		
		2	~~0.804~~	~~1.33~~	~~0.605~~	~~**0.230**~~ **0.183**	~~**68.08**~~ **32.41**
		3	0.296	1.33	0.223		
	EP-FM50.6	1	0.376	1.33	0.283		
		2	0.376	1.33	0.283		
		3	0.224	1.33	0.168		

Appendix B

Table B. 1 Results of three-point bending tests at 23°C with unfilled binder (EP1, EP2)

No	Specimen	Width (mm)	Height (mm)	Elastic modulus (MPa)	Strength (MPa)	Average elastic modulus (MPa)	Average strength (MPa)	Variation coefficient (modulus)	Variation coefficient (strength)	Average density (ton/m³)
1	EP 1.1.3	8.75	3.1	2800	58.9					
2	EP 2.1.1	10.55	3	2140	98					
3	EP 2.1.2	11.8	3.05	2350	62.1					
4	EP 2.2.1	9	2.7	2090	62.3					
5	EP 1.3.2	13.3	3	~~1770~~	72.1	~~**2350**~~ **2398**	~~**65**~~ **60.7**	12.9%	36.6%	1.163
6	EP 1.4.2	13.8	3.6	2720	56.8					
7	EP 3.1	13.8	3.6	2190	33.1					
8	EP 1.1.2	8.3	3	2390	53					
9	ЕРИ 1.2	8	3	2660	48.5					
10	EP 1.2.1	7.25	2.85	2470	66.3					

 doi:10.20944/preprints202211.0377.v1

11	EP 1.4.1	10.25	5.8	2420	81.7					
12	EP 1.9.1	11.1	5.1	2560	36					
13	EP 2.3.2	7.8	5.55	1986	~~120.1~~					

Table B. 2 Results of three-point bending tests at 100°C with unfilled binder (EP1, EP2)

No	Specimen	Width (mm)	Height (mm)	Elastic modulus (MPa)	Strength (MPa)	Average elastic modulus (MPa)	Average strength (MPa)	Variation coefficient (modulus)	Variation coefficient (strength)	Average density (ton/m³)
1	EP 3.2	8.2	5.4	1987	69.9					
2	EP 1.3	10.25	4	2480	75.9					
3	EP 2.3	8.8	5	1702	n/a					
4	EP 1.1.1	6.85	4.75	1993	69					
5	EP 1.1.4	7.1	5	2180	60.3					
6	EP 1.3.1	8	5.1	1790	n/a	~~1866~~ **1970**	**71**	28.1%	11.0%	1.163
7	EP 1.4.3	10.6	5.3	1161	n/a					
8	EP 1.9.3	11.55	4.25	2680	81.1					
9	EP 2.1.3	11.6	5.2	1812	n/a					
10	EP 2.2.2	9	5.4	1822	n/a					
11	EP 2.2.3	7.9	6.9	~~729~~	n/a					
12	EP 2.2.5	8	4.9	2060	n/a					

Table B. 3 Three-point bending test results at 23oC of filled binder (EP-FA25)

No	Specimen	Width (mm)	Height (mm)	Elastic modulus (MPa)	Strength (MPa)	Average elastic modulus (MPa)	Average strength (MPa)	Variation coefficient (modulus)	Variation coefficient (strength)	Average density (ton/m³)
1	FA 25.4.1	8.1	4.05	3260	58.9					
2	FA 25.4.2	8.1	4.9	3140	~~98~~					
3	FA 25.4.3	7.4	4.1	3520	62.1					
4	FA 25.4.4	8.25	4.2	3670	62.3					
5	FA 25.1.1	12	5.675	3690	72.1					
6	FA 25.1.2	9.55	5.5	3360	56.8	**3421**	~~63~~ **62.4**	11.4%	27.2%	1.276
7	FA 25.1.3	13	4.95	3210	~~33.1~~					
8	FA 25.3.1	10.2	5.8	2690	53					
9	FA 25.3.2	6.7	4.55	3540	48.5					
10	FA 25.3.3	9	5	3320	66.3					
11	FA 25.3.4	7.4	4.8	4230	81.7					

Table B. 4 Three-point bending test results at 23°C of filled binder (EP-FA50)

No	Specimen	Width (mm)	Height (mm)	Elastic modulus (MPa)	Strength (MPa)	Average elastic modulus (MPa)	Average strength (MPa)	Variation coefficient (modulus)	Variation coefficient (strength)	Average density (ton/m³)

 doi:10.20944/preprints202211.0377.v1

1	FA 50.4.3	6.45	2.6	5110	65.9					
2	FA 50.3.1	8.9	4.325	5510	69.5					
3	FA 50.3.3	6.75	2.1	5290	64.5					
4	FA 50.3.2	7.25	3.35	6250	68.8					
5	FA 50.4.4	6	4.05	5750	68.4	**5645**	**69**	8.1%	8.6%	1.415
6	FA 50.1.1	5.1	2.15	5300	68.2					
7	FA 50.4.1	8.15	5.35	5300	71.8					
8	FA 50.4.2	5.6	3.85	6080	77.5					
9	FA 50.1.2	4.5	3.725	6430	79.9					
10	FA 50.3.4	5.9	3	5430	59.4					

Table B. 5 Three-point bending test results at 23°C of filled binder (EP-FM33)

No	Specimen	Width (mm)	Height (mm)	Elastic modulus (MPa)	Strength (MPa)	Average elastic modulus (MPa)	Average strength (MPa)	Variation coefficient (modulus)	Variation coefficient (strength)	Average density (ton/m^3)
	FM 2.1	8.65	3.8	5140	84.6					
	FM 2.2	7.2	3.9	3630	75.8					
	FM 1	8.85	5.1	3610	89.7	**4045**	**73**	17.1%	19.5%	1.436
	FM 2	6.95	5.65	4050	51.9					
	FM 5.1	8.05	3.65	4550	61.2					
	FM 3	12.4	3.85	3290	73.4					